Inorg. Chem. **2006**, *45*, 6460–6466

Ferromagnetic Coupling Promoted by κ^3N:κ^2N Bridging System

Asako Igashira-Kamiyama,*,† Takashi Kajiwara,*,‡ Takumi Konno,† and Tasuku Ito‡

Department of Chemistry, Graduate School of Science, Osaka University, Toyonaka, Osaka 560-0043, Japan, and Department of Chemistry, Graduate School of Science, Tohoku University, Aoba, Aramaki, Aoba-ku, Sendai 980-8578, Japan

Received December 7, 2005

Syntheses, structures, and magnetic properties of novel trinuclear complexes of the same motif $[M\{Cu(pz_2bg)_2\}M]^{4+}$ (M = Cu^{II}, Ni^{II}, Co^{II}, Mn^{II}), *catena*-$[Cu_2\{Cu(pz_2bg)_2\}(Hpz)_2(PhSO_3)_2](PhSO_3)_2\cdot 4H_2O$ (**2**·$4H_2O$), $[Ni_2\{Cu(pz_2bg)_2\}(MeOH)_2(H_2O)_4](NO_3)_4$ (**3**), $[Co_2\{Cu(pz_2bg)_2\}(NO_3)_2(EtOH)_2](NO_3)_2$ (**4**), and $[Mn_2\{Cu(pz_2bg)_2\}(NO_3)_4(MeCN)_2]$ (**5**), which include the complex ligand $[Cu(pz_2bg)_2]$ (**1**), are reported (Hpz = pyrazole, pz_2bg^- = di(pyrazolecarbimido)aminate; bispyrazolyl derivative of biguanidate). The reaction of $Cu(ClO_4)_2\cdot 6H_2O$, sodium dicyanamide, Hpz, and $PhSO_3H\cdot H_2O$ (1:2:4:4) in MeOH yielded blue crystals of $[Cu_2(\mathbf{1})(Hpz)_2(PhSO_3)_2](PhSO_3)_2\cdot 4H_2O$ (**2**·$4H_2O$). In **2**, the tricopper(II) units, which consist of two Cu^{II} ions bridged by **1**, are linked by benzenesulfonate anions to form a ladder structure. Complex **1** was isolated by removing the terminal Cu^{II} ions from **2** with use of Na_4edta. Complexes **3**–**5** were obtained by the reaction of **1** with an excess of each M^{II} ion. In **2**–**5**, the adjoining metal ions are ferromagnetically coupled via the pz_2bg^- ligand with *J* values of +7.2(1), +7.5(1), +2.7(1), and +0.3(1) cm^{-1}, respectively, using a spin Hamiltonian $H = -2J(S_{M1}S_{Cu} + S_{Cu}S_{M2})$. The ferromagnetic interaction was attributed to the strict orthogonality of magnetic dσ orbitals, which are controlled by the κ^3N:κ^2N bridging geometry of the pz_2bg^- ligands.

Introduction

Rational synthesis of polynuclear metal clusters with large ground spin states is important for the development of molecular magnets, such as single-molecule magnets and single-chain magnets.[1] Several methods have been proposed to produce ferromagnetic interactions between metal ions[2] including orthogonality of the magnetic orbitals,[3] spin polarization,[4] and double-exchange interactions.[5] Design of the transition metal complexes to achieve strict orthogonality or accidental orthogonality of the magnetic orbitals is the most common way to incorporate ferromagnetic interactions. The strict orthogonality is expected for the combination of metal ions having dσ and dπ spins as found in a Cu^{II} ($d_{x^2-y^2}$)−VO (d_{xy}) system,[3] and the accidental orthogonality often occurs for dσ−dσ orbital pairs when the bridging angle is close to 90°.[6] On the other hand, a ferromagnetic interaction between dπ−dπ spins can be produced by the spin-polarization mechanism. It is rather simple to design metal complexes with ferromagnetic interactions by the combination of dπ−dσ pairs or dπ−dπ pairs using the mechanism of strict orthogonality or spin polarization, as mentioned above. However, in the case of the dσ−dσ spins, it is rather difficult to realize the ferromagnetic coupling by designing the structures since strict control of bridging angles is required.

Recently, we demonstrated that the ferromagnetic interactions between dσ spins were produced with strict orthogonality by controlling the bridging geometry of ligands.[7−9] In a κ^1N:κ^2N bridging mode, two metal $d_{x^2-y^2}$ orbitals have

* To whom correspondence should be addressed. E-mail: igashira@ch.wani.osaka-u.ac.jp (A.I.-K.); kajiwara@agnus.chem.tohoku.ac.jp (T.K.).
† Osaka University.
‡ Tohoku University.

(1) For example, see: (a) *Magnetism: Molecules to Materials III*; Miller, J. S., Drillon, M., Eds.; Wiley VCH: Weinheim, Germany, 2002. (b) Gatteschi, D.; Sessoli, R. *Angew. Chem., Int. Ed.* **2003**, *42*, 268.
(2) Kahn, O. *Molecular Magnetism*; VCH: New York, 1993.
(3) (a) Goodenough, J. B. *Phys. Rev.* **1955**, *100*, 564. (b) Kanamori, J. *J. Phys. Chem. Solids* **1959**, *10*, 87. (c) Kahn, O.; Galy, J.; Jour-nauxd, Y.; Jaid, J.; Morgenstern-Badarau, I. *J. Am. Chem. Soc.* **1982**, *104*, 2165. (d) Torihara, N.; Okawa, H.; Kida, S. *Chem. Lett.* **1978**, 1269.
(4) (a) Fernández, I.; Ruiz, R.; Faus, J.; Julve, M.; Lloret, F.; Cano, J.; Ottenwaelder, X.; Journaux, Y.; Muñoz, M. C. *Angew. Chem., Int. Ed.* **2001**, *40*, 3039. (b) Lloret, F.; de Munno, G.; Julve, M.; Cano, J.; Ruiz, R.; Caneschi, A. *Angew. Chem., Int. Ed.* **1998**, *37*, 135. (c) Oshio, H.; Ichida, H. *J. Phys. Chem.* **1995**, *99*, 3294.
(5) (a) Zener, C. *Phys. Rev.* **1951**, *82*, 403. (b) Anderson, P. W.; Hasegawa, H. *Phys. Rev.* **1955**, *100*, 675. (c) Blondin, G.; Girerd, J.-J. *Chem. Rev.* **1990**, *90*, 1359.
(6) Crawford, V. H.; Richardson, H. W.; Wasson, J. R.; Hodgson, D. J.; Hatfield, W. E. *Inorg. Chem.* **1976**, *15*, 2107.
(7) (a) Kajiwara, T.; Kamiyama, A.; Ito, T. *Chem. Commun.* **2002**, 1256. (b) Kajiwara, T.; Kamiyama, A.; Ito, T. *Polyhedron* **2003**, *22*, 1789.

10.1021/ic0520925 CCC: $33.50
Published on Web 07/12/2006

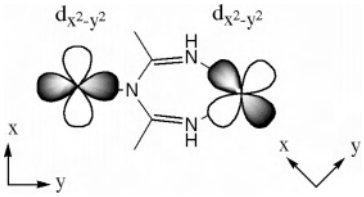

Figure 1. Schematic representation of the $d_{x^2-y^2}$ orbitals in a $\kappa^1N:\kappa^2N$ bridging mode.

different symmetries and are orthogonal to each other, and thus a ferromagnetic interaction occurs between metal ions with dσ spins (Figure 1). The polynuclear complexes constructed from the complex ligand [Cu(bptap)$_2$] (bptap$^-$ = 2,4-bis(2-pyridyl)-1,3,5-triazapentanedienate) with a κ^3N:κ^2N bridging mode show the ferromagnetic interactions between Cu^{II} and M^{II} ions (M = Cu, Ni, and Mn), and [Cu(bptap)$_2$] acts as a ferromagnetic coupler. However, most of the complexes containing [Cu(bptap)$_2$] could not be structurally determined and the magnetostructural studies have not been achieved in detail.

In this paper, we report on the syntheses and structures of novel trinuclear complexes of the same motif [M{Cu(pz$_2$bg)$_2$}M]$^{4+}$ (M = Cu^{II}, Ni^{II}, Co^{II}, Mn^{II}), *catena*-[Cu$_2${Cu(pz$_2$bg)$_2$}(Hpz)$_2$(PhSO$_3$)$_2$](PhSO$_3$)$_2$ (**2**), [Ni$_2${Cu(pz$_2$bg)$_2$}(MeOH)$_2$(H$_2$O)$_4$](NO$_3$)$_4$ (**3**), [Co$_2${Cu(pz$_2$bg)$_2$}(NO$_3$)$_2$(EtOH)$_2$](NO$_3$)$_2$ (**4**), and [Mn$_2${Cu(pz$_2$bg)$_2$}(NO$_3$)$_4$(MeCN)$_2$] (**5**), together with those of a complex ligand [Cu(pz$_2$bg)$_2$] (**1**) (Hpz = pyrazole, pz$_2$bg$^-$ = di(pyrazolecarbimido)aminate; bispyrazolyl derivative of biguanidate). The ferromagnetic properties of those trinuclear complexes, which indicate that the complex ligand **1** acts as a ferromagnetic coupler, are also reported.

Experimental Section

All solvents and chemicals were purchased as reagent grade and used without further purification. Fourier transform infrared spectroscopy was performed on a JASCO FT/IR-620 instrument as KBr pellets. Variable-temperature magnetic susceptibility measurements were made using a SQUID magnetometer MPMS 5S (Quantum Design) at 1 T for **2** and 0.5 T for **3**, **4**, and **5**. The diamagnetic correction for each sample was determined from Pascal's constants.

Synthesis of *catena*-[Cu$_2${Cu(pz$_2$bg)$_2$}(Hpz)$_2$(PhSO$_3$)$_2$](PhSO$_3$)$_2$·4H$_2$O (2·4H$_2$O). The addition of a solution containing sodium dicyanamide (190 mg, 2 mmol) in MeOH (5 mL) to a solution of Cu(ClO$_4$)$_2$·6H$_2$O (370 mg, 1 mmol) in MeOH (5 mL) produced a green precipitate. To the resulting suspension, a solution containing both pyrazole (270 mg, 4 mmol) and PhSO$_3$H·H$_2$O (700 mg, 4 mmol) in MeOH (5 mL) was added, and then the green precipitate was dissolved. This green solution was stood at room-temperature overnight, during which the color of solution changed to blue, and complex **2**·4H$_2$O was obtained as blue crystals after several days, which were filtered and dried in the air (270 mg, 0.19 mmol, 56%). Anal. Calcd for Cu$_3$C$_{46}$H$_{52}$N$_{18}$O$_{16}$S$_4$ (**2**·4H$_2$O): C, 38.59; H, 3.66; N, 17.61; C/N, 2.56. Found: C, 38.14; H, 3.67; N, 17.49; C/N, 2.54. IR (KBr disk, cm^{-1}): ν(CN) 1656 (s).

Synthesis of [Cu(pz$_2$bg)$_2$] (1). Compound **2**·4H$_2$O (300 mg, 0.22 mmol) and Na$_4$edta (500 mg, 1.3 mmol) were vigorously stirred for 2 h in a H$_2$O (20 mL)/CHCl$_3$ (20 mL) mixture at room temperature. The purple organic layer was separated and evaporated to dryness. Pale red crystals of **1** were obtained by recrystallization from EtOH/CHCl$_3$ (94 mg, 0.2 mmol, 91%). Anal. Calcd for CuC$_{16}$H$_{16}$N$_{14}$ (**1**): C, 41.07; H, 3.45; N, 41.91; C/N, 1.14. Found: C, 40.98; H, 3.23; N, 41.50; C/N, 1.15. IR (KBr disk, cm^{-1}): ν(CN) 1625 (s).

Synthesis of [Ni$_2${Cu(pz$_2$bg)$_2$}(MeOH)$_2$(H$_2$O)$_4$](NO$_3$)$_4$ (3). A solution of **1** (5 mg, 0.01 mmol) in CHCl$_3$ (2 mL) was added to a solution of Ni(NO$_3$)$_2$·6H$_2$O (29 mg, 0.1 mmol) in MeOH (1 mL)/acetone (8 mL). Pale purple plates of **3** were formed from the resulting purple solution by slow evaporation at room temperature, which were collected and dried in the air (~50%). Anal. Calcd for Ni$_2$CuC$_{18}$H$_{32}$N$_{18}$O$_{18}$ (**3**): C, 22.30; H, 3.33; N, 26.00; C/N, 1.00. Found: C, 22.85; H, 3.13; N, 26.18; C/N, 1.02. IR (KBr disk, cm^{-1}): ν(CN) 1698 (w), 1652 (s), ν(NO$_3^-$) 1286 (s).

Synthesis of [Co$_2${Cu(pz$_2$bg)$_2$}(NO$_3$)$_2$(EtOH)$_2$](NO$_3$)$_2$ (4). A solution of **1** (5 mg, 0.01 mmol) in CHCl$_3$ (2 mL) was added to a solution of Co(NO$_3$)$_2$·6H$_2$O (29 mg, 0.1 mmol) in EtOH (1 mL)/acetone (8 mL). Both pale red large plates of **4** and small plates of **4′**[11] were obtained by slow evaporation at room temperature, which were separated by hand and dried in air (~ 10%). Anal. Calcd for Co$_2$CuC$_{20}$H$_{28}$N$_{18}$O$_{14}$ (**4**): C, 25.94; H, 3.05; N, 27.23; C/N, 1.11. Found: C, 26.10; H, 3.00; N, 26.98; C/N, 1.13. IR (KBr disk, cm^{-1}): ν(CN) 1697 (w), 1650 (s), ν(NO$_3^-$) 1286 (s).

Synthesis of [Mn$_2${Cu(pz$_2$bg)$_2$}(NO$_3$)$_4$(MeCN)$_2$] (5). A solution of **1** (5 mg, 0.01 mmol) in CHCl$_3$ (2 mL) was added to a solution of Mn(NO$_3$)$_2$·6H$_2$O (29 mg, 0.1 mmol) in MeOH (1 mL)/MeCN (8 mL). Complex **5** was obtained as pale red plates by slow evaporation at room temperature, collected, and dried in air (~10%). Anal. Calcd for Mn$_2$CuC$_{20}$H$_{22}$N$_{20}$O$_{12}$ (**5**): C, 26.46; H, 2.44; N, 30.85; C/N, 1.00. Found: C, 26.31; H, 2.50; N, 31.11; C/N, 0.97. IR (KBr disk, cm^{-1}): ν(CN) 1633 (s), ν(NO$_3^-$) 1286 (s).

Crystal Structure Analyses. X-ray data for all complexes were collected at low temperature (200 K to 223 K) with a Bruker AXS SMART-1000/CCD area detector using graphite-monochromated Mo Kα radiation. The intensity data were empirically corrected for absorption with using the program SADABS.[12] The structures were solved by direct methods using SIR97,[13] SIR92,[14] and the structure refinements were carried out using full-matrix least-squares (SHELXL-97).[15] Non-hydrogen atoms, except for some solvent molecules, were refined anisotropically, while the hydrogen atoms, except for the imino groups (C=NH), were treated using a riding

(8) (a) Kamiyama, A.; Noguchi, T.; Kajiwara, T.; Ito, T. *CrystEngComm* **2003**, *5*, 231. (b) Kamiyama, A.; Noguchi, T.; Kajiwara, T.; Ito, T. *Inorg. Chem.* **2002**, *41*, 507. (c) Kajiwara, T.; Nakano, M.; Kaneko, Y.; Takaishi, S.; Ito, T.; Yamashita, M.; Igashira-Kamiyama, A.; Nojiri, H.; Ono, Y.; Kojima, N. *J. Am. Chem. Soc.* **2005**, *127*, 10150. (d) Kajiwara, T.; Sensui, R.; Noguchi, T.; Kamiyama, A.; Ito, T. *Inorg. Chim. Acta* **2002**, *337*, 299. (e) Kamiyama, A.; Noguchi, T.; Kajiwara, T.; Ito, T. *Angew. Chem., Int. Ed.* **2000**, *39*, 3130. (f) Kajiwara, T.; Ito, T. *J. Chem. Soc., Dalton Trans.* **1998**, 3351.

(9) Tong, M.-L.; Wu, Y.-M.; Tong, Y.-X.; Chen, X.-M.; Chang, H.-C.; Kitagawa, S. *Eur. J. Inorg. Chem.* **2003**, 2385.

(10) (a) Cohn, G. *J. Prakt. Chem.* **1911**, *84*, 394. (b) Rembarz, G.; Brandner, H.; Finger, H. *J. Prakt. Chem.* **1964**, *26*, 314.

(11) **4′** is also a trinuclear Co^{II}Cu^{II}Co^{II} complex, [Co$_2${**1**}(NO$_3$)$_4$(EtOH)$_2$], in which each Co^{II} ion is in a N$_3$O$_3$ octahedral coordination geometry from **1**, two monodentate nitrate ions, and one EtOH molecule.

(12) Sheldrick, G. M. *SADABS. Program for Empirical Absorption Correction of Area Detector Data*; University of Göttingen: Göttingen, Germany, 1996.

(13) For SIR97, see: Altomare, A.; Cascarano, G.; Giacovazzo, C.; Guagliardi, A.; Moliterni, A. G. G.; Burla, M. C.; Polidori, G.; Camalli, M.; Spagna, R. *J. Appl. Crystallogr.* **1999**, *32*, 115.

(14) Altomare, A.; Burla, M. C.; Camalli, M.; Cascarano, M.; Giacovazzo, C.; Guagliardi, A.; Polidori, G. *J. Appl. Crystallogr.* **1994**, *27*, 435.

(15) Sheldrick, G. M. *SHELXL97. Program for the Refinement of Crystal Structures*; University of Göttingen: Göttingen, Germany, 1997.

Scheme 1. Syntheses of Complexes **1**, **2**, **3**, **4**, and **5**

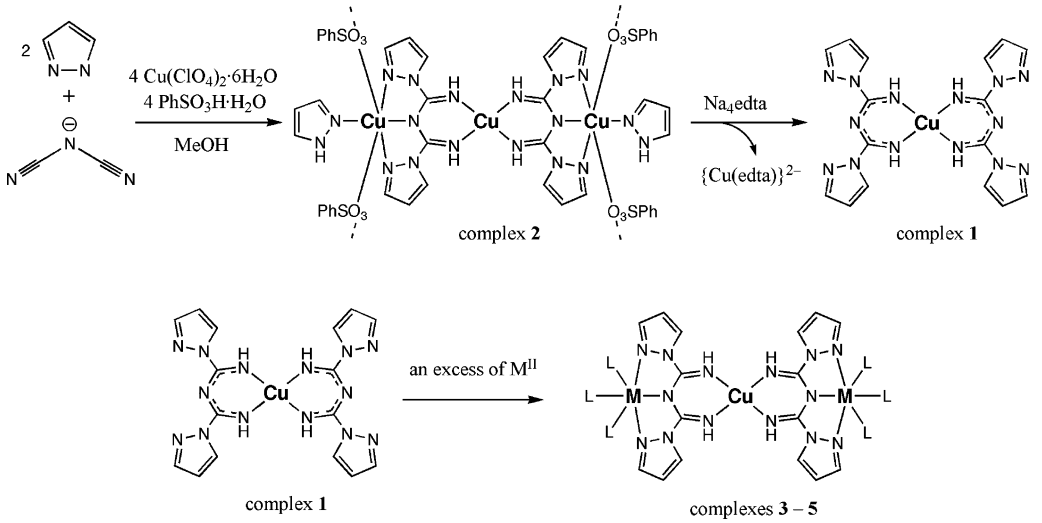

Table 1. Crystallographic Data for **1**, **2**·4H_2O, **3**, **4**, and **5**

	1	**2**·4H_2O	**3**	**4**	**5**
formula	$C_{16}H_{16}CuN_{14}$	$C_{46}H_{52}Cu_3N_{18}O_{16}S_4$	$C_{18}H_{32}CuN_{18}Ni_2O_{18}$	$C_{20}H_{28}Co_2CuN_{18}O_{14}$	$C_{20}H_{22}CuMn_2N_{20}O_{12}$
fw	467.97	1431.92	969.58	926.00	908.00
cryst syst	triclinic	triclinic	triclinic	triclinic	triclinic
space group	$P\bar{1}$	$P\bar{1}$	$P\bar{1}$	$P\bar{1}$	$P\bar{1}$
a (Å)	6.0334(10)	7.3523(8)	7.9540(11)	7.4835(8)	7.6584(11)
b (Å)	7.4286(12)	14.6970(15)	9.2830(13)	7.8475(8)	8.3806(13)
c (Å)	10.8672(18)	14.8462(15)	13.5000(19)	14.6737(15)	14.769(2)
α (deg)	93.404(3)	78.423(4)	78.113(3)	88.546(2)	80.457(4)
β (deg)	102.036(3)	77.953(4)	72.845(3)	82.726(2)	75.121(4)
γ (deg)	93.295(3)	76.328(4)	70.592(3)	84.276(2)	63.311(4)
V (Å^3)	474.30(13)	1505.0(3)	891.9(2)	850.47(15)	817.1(2)
Z	1	1	1	1	1
T (K)	223(2)	200(2)	223(2)	223(2)	213(2)
ρ_{calcd} (g cm^{-3})	1.638	1.580	1.805	1.808	1.845
μ (mm^{-1})	1.191	1.269	1.736	1.676	1.499
R1 [$I > 2\sigma(I)$][a]	0.0361	0.0522	0.0548	0.0357	0.0403
wR2 [$I > 2\sigma(I)$][b]	0.0757	0.1080	0.1221	0.0780	0.0935
R1 [all data][a]	0.0452	0.1156	0.0794	0.0490	0.0602
wR2 [all data][b]	0.0778	0.1193	0.1316	0.0822	0.0996

[a] $R1 = \sum||F_o| - |F_c||/\sum|F_o|$. [b] $wR2 = [\sum w(F_o^2 - F_c^2)^2/\sum w(F_o^2)^2]^{1/2}$.

model. The hydrogen atoms attached to $N_{C=NH}$ were located from the difference Fourier map and refined isotropically.

Results and Discussion

Syntheses. The synthesis of complex **2** containing two pz_2bg^- ligands was performed by the nucleophilic addition of a secondary amine (pyrazole, Hpz) to the cyano groups of dicyanamidate in the presence of the Cu^{II} ion and acid (Scheme 1).[10] This method is similar to that reported in a previous paper, except for the addition of acid.[9] Complex **1** was obtained by extracting the terminal Cu ions from the trinuclear complex **2** with use of edta^{4-}. Complex **1** has six free nitrogen atoms, which have the ability to coordinate to other metal ions; hence, **1** can be used as a bistridentate complex ligand. When complex **1** was allowed to react with M^{II} in a 1:2 molar ratio, insoluble precipitates immediately appeared. The IR spectra of the precipitates indicate the coordination of pyrazolyl sites in **1** to M^{II} ions, and 1D polynuclear chain species consisting of **1** and M^{II} are thought to be formed. To avoid the formation of insoluble precipitates, an excess of M^{II} was reacted with **1**, leading to the formation of crystals of the desirable trinuclear complexes. The choice of solvents is also important to grow crystals suitable for X-ray analysis.

Structures. Mononuclear complex **1** and trinuclear complexes **2**, **3**, **4**, and **5** have been characterized by single-crystal X-ray analyses. The crystallographic data are summarized in Table 1, and the selected atom···atom distances are summarized in Table 2.

Figure 2 shows the structure of mononuclear complex **1**. Complex **1** crystallizes in the space group $P\bar{1}$, and the asymmetric unit consists of one-half of the complex molecule. The Cu^{II} ion is located on a crystallographic inversion center. The Cu^{II} ion is in a square-planar coordination environment with four $N_{C=NH}$ atoms from two chelating pz_2bg^- ligands with Cu−N distances of 1.919(2) and 1.925(2) Å. The $C-N_{amide}$ distances are 1.327(3) and 1.325(3) Å, while those of $C-N_{C=NH}$ are 1.300(3) and 1.298(3) Å. The small difference in bond distances between $C-N_{amide}$ and $C-N_{C=NH}$ indicates that the negative charge on the pz_2bg^- ligand is delocalized on the whole N−C−N−C−N conjugated system. The N_{pz} atoms (N1 and N5)

Table 2. Selected Atom−Atom Distances (Å) for **1**, **2**·4H_2O, **3**, **4**, and **5**

	1	2	3	4	5
Cu1−N6	1.919(2)	1.953(6)	1.944(3)	1.952(2)	1.952(3)
Cu1−N7	1.925(2)	1.962(6)	1.953(3)	1.954(2)	1.938(2)
N3−C4	1.327(3)	1.338(7)	1.352(5)	1.342(3)	1.347(3)
N3−C5	1.325(3)	1.325(7)	1.343(5)	1.349(3)	1.335(4)
N6−C4	1.300(3)	1.300(8)	1.289(5)	1.284(3)	1.284(4)
N7−C5	1.298(3)	1.287(8)	1.285(5)	1.278(3)	1.285(4)
M−N3[a]		1.962(4)	2.026(3)	2.064(2)	2.302(2)
M−N1[a]		1.981(5)	2.051(4)	2.100(2)	2.211(3)
M−N5[a]		1.977(5)	2.051(3)	2.071(2)	2.217(2)
M−X_A[a,b]		1.966(4)	2.033(3)	2.200(2)	2.318(2)
					2.292(2)
M−X_B[a,c]		2.488(4)	2.082(4)	2.032(2)	2.254(2)
		2.497(4)	2.108(3)	2.143(2)	2.264(3)
Cu···M[a]		5.2666(8)	5.3459(8)	5.3975(5)	5.6428(8)

[a] M = Cu^{II} (**2**), Ni^{II} (**3**), Co^{II} (**4**), and Mn^{II} (**5**). [b] X_A shows a coordinating atom in the pz_2bg^- plane (N_{pz} (**2**), O_{water} (**3**), O_{NO3} (**4**), and O_{NO3} (**5**)). [c] X_B shows coordinating atoms out of the pz_2bg^- plane (O_{BzSO3} (**2**), O_{water} and O_{MeOH} (**3**), O_{NO3} and O_{EtOH} (**4**), and O_{NO3} and N_{MeCN} (**5**)).

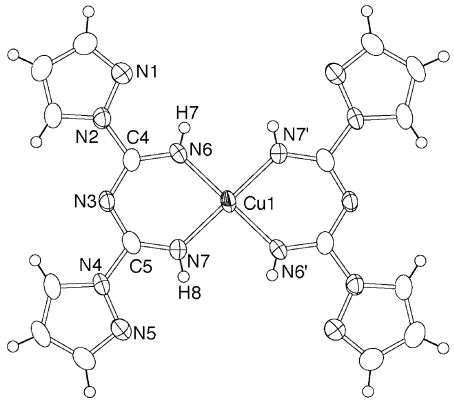

Figure 2. ORTEP drawings of **1** with thermal ellipsoids at 50% probability. Symmetry codes: (′) $-x + 1, -y + 1, -z + 2$.

are directed toward $N_{C=NH}$ (N6−H7 and N7−H8, respectively) to form hydrogen bonds with N···H distances of 2.25 and 2.28 Å, respectively.

Complex **2** has a ladder structure consisting of tricopper(II) units $\{Cu_2\{\mathbf{1}\}(Hpz)_2\}^{4+}$ bridged by benzenesulfonate anions, as shown in Figure 3. This complex crystallizes in the space group $P\bar{1}$, and a half of the tricopper(II) unit, one benzenesulfonate, and water molecules are crystallographically independent. The tricopper(II) unit consists of two terminal Cu^{II} ions (Cu2 and Cu2′) and a bridging {**1**} unit that involves Cu1. The central Cu^{II} ion (Cu1) is in a square planar coordination geometry surrounded by four $N_{C=NH}$ atoms from two pz_2bg^- ligands in a κ^2N mode (Cu−N = 1.953(6) and 1.962(6) Å). Each of the terminal Cu^{II} ions is situated in an axially elongated octahedron coordinated by three N atoms from a pz_2bg^- ligand (in a κ^3N mode) and one pyrazole N atom in an equatorial plane (Cu−N = 1.962(4)−1.981(5) Å), and two O atoms from benzenesulfonate ions in axial positions (Cu−O = 2.488(4) and 2.497(4) Å). The structure of the tricopper(II) unit is similar to that of a related tricopper(II) complex reported previously.[9] The coordination geometry of the three Cu^{II} ions indicates that the magnetic orbital of each Cu^{II} ion is $d_{x^2-y^2}$, which involves the basal four donors (Figure 6a).

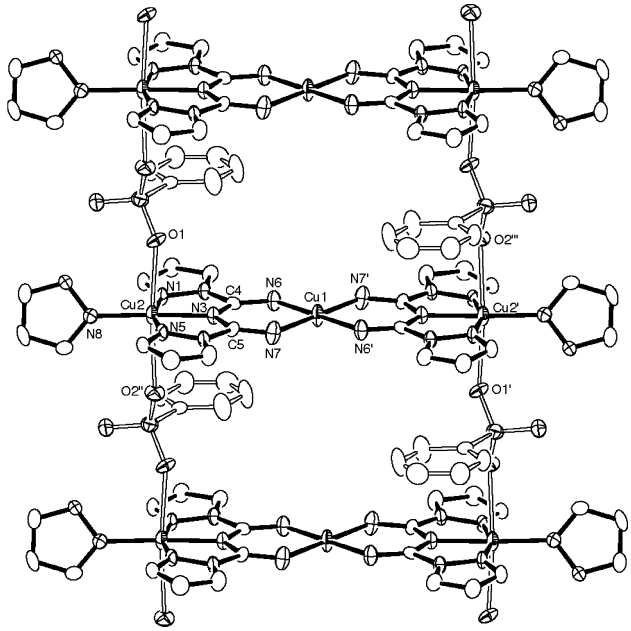

Figure 3. ORTEP drawings of cationic part of **2** with thermal ellipsoids at 50% probability. Hydrogen atoms are omitted for clarity. The trinuclear $\{Cu_2\{Cu(pz_2bg)_2\}(Hpz)_2\}^{4+}$ units are represented with solid bonds, whereas the bridging benzenesulfonate ions are represented with open bonds. Symmetry codes: (′) $-x + 1, -y + 2, -z + 2$; (″) $x + 1, y, z$; (‴) $-x, -y + 2, -z + 2$.

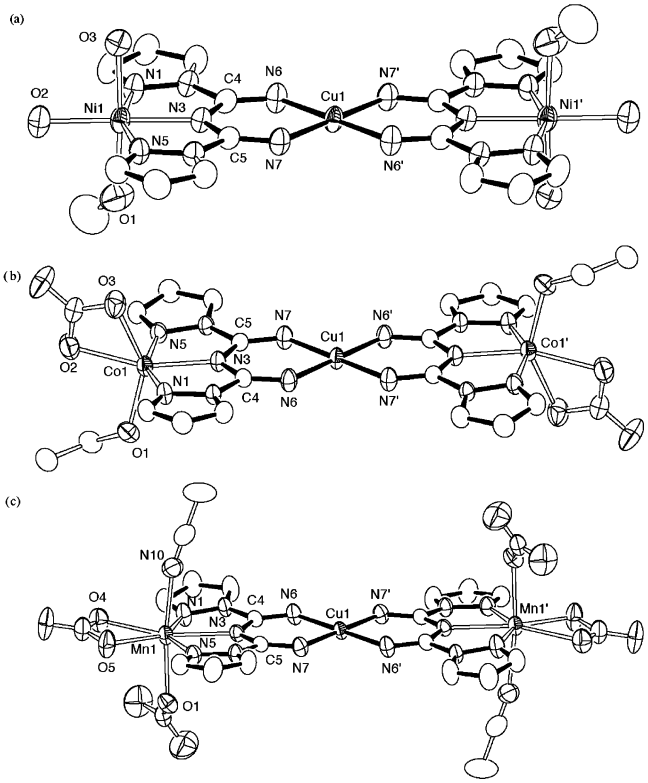

Figure 4. ORTEP drawings of the cationic parts of **3** (a) and **4** (b) and all of **5** (c) with thermal ellipsoids at 50% probability. Hydrogen atoms are omitted for clarity. The moiety with the solid bonds represents the {**1**} unit. Symmetry codes: (′) $-x + 1, -y + 1, -z + 2$ (**3**); $-x + 2, -y, -z$ (**4**); $-x, -y + 2, -z$ (**5**).

The crystal structures of the trinuclear complexes **3**, **4**, and **5** are shown in Figure 4. All of the complexes crystallized in the same space group, $P\bar{1}$. The central Cu^{II} ion in each complex is located on a crystallographic inversion center

and one-half of the trinuclear complex is crystallographically independent. Two M^{II} ions (Ni^{II} (**3**), Co^{II} (**4**), and Mn^{II} (**5**)) are linked by a {**1**} moiety, which acts as a bridging bistridentate complex ligand, forming a linear trinuclear structure.

Complex **3** consists of the trinuclear cationic part and four nitrate ions as counteranions. In **3**, the complex ligand **1** coordinates to two Ni^{II} ions via N_3 sites with distances of 2.026(3), 2.051(3), and 2.051(4) Å, and three O atoms from one MeOH (O1, Ni−O = 2.082(4) Å) and two water molecules (O2 and O3, Ni−O = 2.033(3) and 2.108(3) Å) are bound to each Ni^{II} ion to complete the hexacoordination. The Ni^{II} ion is in a slightly compressed octahedral coordination geometry along the N3−Ni−O2 axis. A high-spin Ni^{II} ion possesses two spins on the e_g orbitals, of which one is directed toward the compressed axis (d_{z^2}), and the other is toward the N_2O_2 equatorial plane ($d_{x^2-y^2}$) shown in Figure 6b. The central Cu^{II} ion is in a square-planar coordination geometry, and its magnetic orbital is $d_{x^2-y^2}$ which is directed toward the four donor N atoms.

Complex **4** involves a dicationic trinuclear part and two nitrate anions. In **4**, two Co^{II} ions are in a hexacoordination with three N donors from a {**1**} unit (Co−N = 2.064(2)−2.100(2) Å), one O donor from a coordinating ethanol molecule (O1, Co−O = 2.032(2) Å), and two O donors from a chelating nitrate anion (O2 and O3, Co−O = 2.143(2) and 2.200(2) Å). Since the chelating angle of the nitrate anion is considerably smaller than 90° (58.27(7)°), the coordination geometry of each Co^{II} ion is highly distorted from a regular octahedron. The magnetic orbitals of each Co^{II} ion are estimated to be d_{z^2}, $d_{x^2-y^2}$, and one of $d\pi$ orbitals (vide infra).

The neutral trinuclear complex **5** consists of two Mn^{II} ions bridged by a bistridentate {**1**} moiety, four coordinating nitrate anions, and two axially coordinating acetonitrile molecules. The Mn^{II} ion is in a distorted pentagonal-bipyramidal environment with three N donors from a {**1**} unit (Mn−N = 2.211(3)−2.302(2) Å) and two O donors from a chelating nitrate anion (O4 and O5, Mn−O = 2.318(2) and 2.292(2) Å) in the equatorial plane, while an N donor from an acetonitrile (N10, Mn−N = 2.264(3) Å) and an O donor from a nitrate anion (O1, Mn−O = 2.254(2) Å) occupy the axial positions. The bond angles in the equatorial N_3O_2 plane of Mn^{II} are in the range of 55.30(8)−84.31(9)°, which is deviated from the ideal angle of a pentagon (72°).

Magnetic Properties. Temperature-dependent magnetic susceptibilities of complexes **2**−**5** were measured down to 2.0 K and are shown in Figure 5. In all complexes, the $\chi_M T$ values increase as the temperature is lowered, suggesting the presence of a ferromagnetic interaction between adjoining metal ions via the pz_2bg^- ligand.

The $\chi_M T$ values for **2** are constant with a value of ca. 1.26 cm^3 K mol^{-1} down to 30 K, which is slightly larger than the spin only value of 1.18 cm^3 K mol^{-1} for three Cu^{II} ions ($S = 1/2$) with an average $g = 2.05$. When the temperature is lowered, the $\chi_M T$ values increase gradually, reaching a maximum value of 1.81 cm^3 K mol^{-1} at 4 K, and then they decrease rapidly. This temperature-dependent behavior of the $\chi_M T$ values at low temperature would be mainly caused by the presence of an antiferromagnetic interaction between the

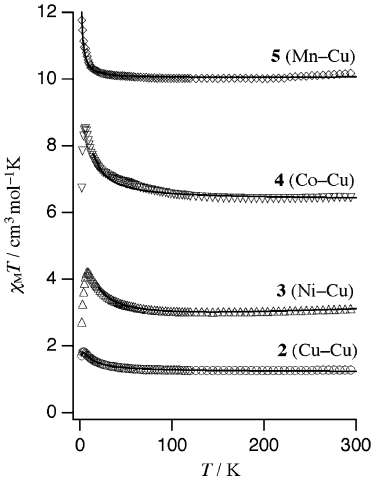

Figure 5. Plots of $\chi_M T$ vs T for **2** (○), **3** (△), **4** (▽), and **5** (◇). Solid line corresponds to the theoretical curve for which parameters are given in the text.

trinuclear units through bridging benzenesulfonate anions. The temperature dependence of $\chi_M T$ was analyzed by the isolated three-spin model ($H = -2J(S_{Cu2}S_{Cu1} + S_{Cu1}S_{Cu2'})$) including θ as the interaction between trinuclear units through bridging benzenesulfonate anions. The best fit parameters were estimated as $J = +7.2(1)$ cm^{-1} and $\theta = -0.3(1)$ K with an averaged g value of 2.05(1).

For **3**, the $\chi_M T$ values are constant with a value of ca. 3.0 cm^3 K mol^{-1} down to 70 K, which is slightly larger than the spin-only value of 2.67 cm^3 K mol^{-1} for dilute three magnetic centers ($S = 1/2$ for Cu^{II} and $S = 1$ for Ni^{II}) with an average g value of 2.12. When the temperature is lowered, the $\chi_M T$ values increase to 4.21 cm^3 K mol^{-1} at 8 K, showing the presence of ferromagnetic coupling between the Cu^{II} and Ni^{II} ions. The swift decrease of the $\chi_M T$ values at low temperature is mainly the result of the zero-field splitting of the Ni^{II} ions. Magnetic data were analyzed with the exchange coupling constant J ($H = -2J(S_{Ni1}S_{Cu} + S_{Cu}S_{Ni2})$) above the temperature of 20 K to avoid the influence of the zero-field splitting. The least-squares calculation yielded best fit parameters of $g = 2.12(1)$ and $J = +7.5(1)$ cm^{-1}.

In **4**, the $\chi_M T$ value at 300 K (6.44 cm^3 K mol^{-1}) is consistent with the spin-only value of 6.37 cm^3 K mol^{-1} for dilute three magnetic centers if the g values are assumed to be 2.53 for g_{Co} and 2.00 for g_{Cu}. When the temperature is lowered, the $\chi_M T$ values retain, gradually increase below 80 K, reach 8.51 cm^3 K mol^{-1} at 6 K, and then decrease rapidly. The swift decrease of $\chi_M T$ values at low temperature is again construed in terms of the zero-field splitting of Co^{II} ions. The best fit parameters of $J = +2.1(1)$ cm^{-1}, $g_{Co} = 2.53(1)$, and $g_{Cu} = 2.00$ (fixed) were obtained with the least-squares fitting for $H = -2J(S_{Co1}S_{Cu} + S_{Cu}S_{Co2})$ above the temperature of 20 K to avoid the influence of the zero-field splitting.

The $\chi_M T$ values for **5** are almost constant with a value of ca. 10.2 cm^3 K mol^{-1} down to 20 K, and they increase to the maximum value of 12.14 cm^3 K mol^{-1} at 2 K. The best fit parameters of $J = +0.3(1)$ cm^{-1} and $g = 2.10(1)$ were obtained for the Hamiltonian of $H = -2J(S_{Mn1}S_{Cu} + S_{Cu}S_{Mn2})$.

In all of the trinuclear complexes, a ferromagnetic coupling occurs which is explained by the orthogonality of magnetic

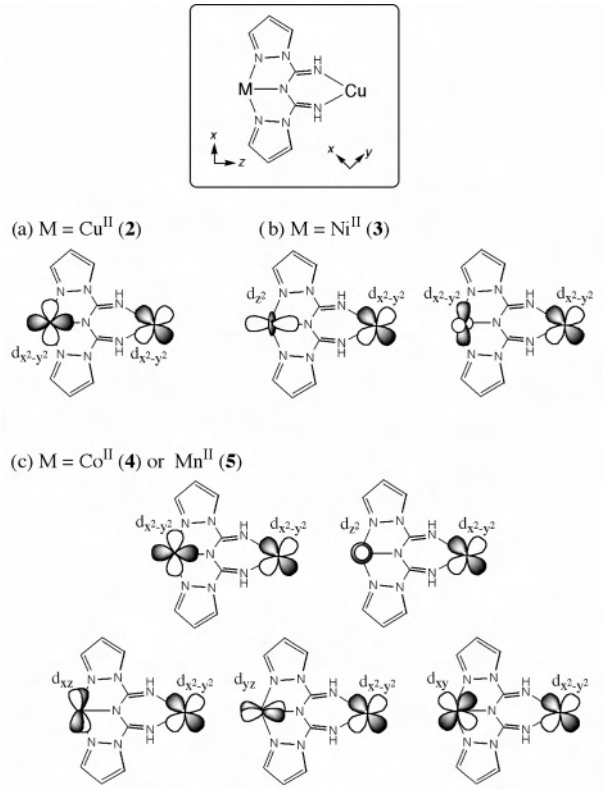

Figure 6. Schematic representation of the magnetic orbitals.

orbitals as expected. The neighboring metal ions are linked by a pz_2bg^- ligand in a $\kappa^2N:\kappa^3N$ fashion, and hence the coordination square plane of the $Cu_{central}$ ion with a κ^2N mode is rotated by 45° relative to that of the $M_{terminal}$ ions with a κ^3N mode. In this bridging mode, the $e_g(Cu_{central})$ and $e_g(M_{terminal})$ orbitals have different symmetries about 2-fold rotation around the $M_{terminal}-Cu_{central}-M_{terminal}$ axis which is advantageous to the ferromagnetic interaction. On the other hand, the $e_g(Cu_{central})$ and $t_{2g}(M_{terminal})$ are symmetric with respect to rotation around the 2-fold axis and have a nonzero overlap integral, which leads to the antiferromagnetic interaction. The net magnetic interaction comes from the sum of these two opposite interactions.

Figure 6 summarizes the magnetic orbitals for each M−Cu pair. In the case of complex **2** (Cu−Cu), the magnetic orbitals of both central and terminal Cu^{II} ions are $d_{x^2-y^2}$, and these orbitals possess different symmetry about a 2-fold rotation axis along Cu^{II}−Cu^{II}−Cu^{II} (i.e., the $Cu_{central}$ is antisymmetric, whereas the $Cu_{terminal}$ is symmetric), and hence, the magnetic orbitals are orthogonal to each other. Similar magnetic interactions have been found in the Cu^{II}−Cu^{II}−Cu^{II} systems reported in previous papers.[7a,9] In complex **3** (Ni−Cu), the magnetic orbitals of the terminal Ni^{II} ions ($d_{x^2-y^2}$ and d_{z^2}) are symmetric about 2-fold axis, whereas the magnetic orbital of the central Cu^{II} ion is antisymmetric, which leads to the ferromagnetic coupling resulting from the orthogonality of the orbitals. The situation is more complicated for complexes **4** (Co−Cu) and **5** (Mn−Cu), since Co^{II} and Mn^{II} ions have both dσ spins on e_g orbitals and dπ spins on t_{2g} orbitals (Figure 6c). However, the t_{2g} orbitals of Co and Mn do not participate in the M−N bonds, and the magnetic interaction between $e_g(Cu_{central})$ and $t_{2g}(M_{terminal})$ should be of the through-space type. This type of interaction is weaker than the through-bond interactions found for the $e_g(Cu_{central})-e_g(M_{terminal})$ pairs, which is predominant in the net ferromagnetic interaction observed for **4** and **5**.

The ferromagnetic interactions in **2** and **3** are rather strong, considering the metal−metal distances (longer than 5 Å), while those for **4** and **5** become weaker and weaker in this order. There are three possible reasons to explain this trend. Since the dσ spins from the metal ions delocalize into the ligand orbitals in some degrees, the dominant magnetic interaction is mediated by direct bonding through the N−C−N−C−N moiety. As the energy separation between the metal d orbital and the ligand level increases, that is, as the energy matching becomes less effective in the order of Cu^{II}, Ni^{II}, Co^{II}, and Mn^{II}, the spin delocalization from a metal ion to a ligand orbital decreases in the same order. As a result, stronger ferromagnetic couplings occur in **2** and **3**. A stronger interaction is expected for **2** with shorter metal−N distances, compared with **3**. However, the observed interactions are almost the same in magnitude for these two complexes. This might be caused by the shape of the magnetic orbitals (i.e., the d_{z^2} orbital in Ni^{II} ion overlaps with the N_{amide} orbital better than the $d_{x^2-y^2}$ orbital in Cu^{II} ion, which compensates for the less matching of the energy levels between Ni^{II} and ligand orbitals, compared with the levels between Cu^{II} and ligand orbitals). Second, the number of the dπ spins on the $M_{terminal}$ site should affect the magnitude of magnetic interactions. As mentioned above, the dσ orbital in the $Cu_{central}$ site and the dπ orbitals in $M_{terminal}$ site have a nonzero overlap integral, which leads to an antiferromagnetic coupling. In **2** and **3**, the $M_{terminal}$ ions have only dσ spin(s) on e_g orbital(s), and a relatively strong ferromagnetic interaction occurs. However, in **4** and **5**, the M^{II} ions have both dσ and dπ spins, which leads to a weaker ferromagnetic interaction relative to **2** and **3**. Finally, in complex **5**, the long Mn^{II}−N bond distances (ca. 2.2 Å) cause the weakest magnetic interaction in these trinuclear complexes.

Conclusion

In this study, we have demonstrated the construction of four linear trinuclear complexes involving the same motif $[M\{Cu(pz_2bg)_2\}M]^{4+}$ (M = Cu^{II} (**2**), Ni^{II} (**3**), Co^{II} (**4**), and Mn^{II} (**5**)). These trinuclear complexes contain a novel complex ligand $[Cu(pz_2bg)_2]$ (**1**) that is regarded as a ferromagnetic coupler. In all the trinuclear complexes, ferromagnetic interactions are observed between neighboring metal ions because of the strict orthogonality of magnetic orbitals. The ferromagnetic interactions arise from the controlled bridging geometry of the $\kappa^2N:\kappa^3N$ mode of the pz_2bg^- ligand. The strength of the interaction is systematically changed when the terminal metal ions are exchanged from Cu^{II} to Ni^{II}, Co^{II}, and Mn^{II} ions, and this tendency is explained in terms of the energy matching of the metal/ligand orbital levels as well as the number of dπ/dσ spins. This kind of orbital orthogonality is generally expected for all combinations of metal ions containing dσ spins, and thus this study showed that the complex ligand **1** is a useful

ferromagnetic coupler for the construction of multinuclear complexes with large ground spin states.

Acknowledgment. This work was supported by a Grant-in-Aid for Scientific Research on Priority Areas (50201497) from the Ministry of Education, Culture, Sports, Science, and Technology, Japan, as well as by JSPS Research Fellowships for Young Scientists (12006281)

Supporting Information Available: X-ray crystallographic files, in CIF format, for the structure determinations of **1**, **2**·4H_2O, **3**, **4**, and **5** and a figure of the structure of **4′** (PDF file). This material is available free of charge via the Internet at http://pubs.acs.org.

IC0520925